Scaling considerations for the application of the sCO2-HeRo system in nuclear power plants

Hacks, Alexander Johannes; Brillert, Dieter

In: 2nd European sCO2 Conference 2018

DOI: https://doi.org/10.17185/duepublico/46089

URN: urn:nbn:de:hbz:464-20180827-132523-4

Link: https://duepublico.uni-duisburg-essen.de:443/servlets/DocumentServlet?id=46089

2nd European supercritical CO2 Conference
August 30-31, 2018, Essen, Germany

2018-sCO2.eu-116

SCALING CONSIDERATIONS FOR THE APPLICATION OF THE SCO2-HERO SYSTEM IN NUCLEAR POWER PLANTS

Alexander Hacks
University of Duisburg-Essen
Duisburg, Germany
Email: Alexander.Hacks@uni-due.de

Dieter Brillert
University of Duisburg-Essen
Duisburg, Germany

ABSTRACT

The supercritical CO_2 heat removal system (sCO2-HeRo) project aims to develop and test a safety system for nuclear power plants with boiling water reactor (BWR) and pressurized water reactor (PWR) reactors for the case of a station blackout with loss of the ultimate heat sink. The safety system is based on a closed Brayton cycle using supercritical CO_2 (sCO2) as working fluid. The project focuses on the experimental proof of the concept and thereby reaching Technology Readiness Level 3 (TRL 3). As the demonstration cycle has a heat source of 200 kW only, the developed turbomachine for the demonstration cycle is a small-scale model. The system in the nuclear power plant (sCO2-NPP) needs to remove up to 60 MW_{th} leading to larger component sizes. The paper shall give an insight in the steps and considerations to proceed from the small-scale model to the actual safety system in the NPP. This includes the evaluation of the aerodynamic efficiency of the turbomachine and the windage losses. Furthermore, concepts of the bearings and generator cooling are investigated regarding possible improvements and required modifications.

INTRODUCTION

Cycles using sCO2 as working fluid have attracted considerable attention due to their compactness and proposed thermodynamic efficiency. The application in a back-up safety system for NPPs however is unique. Most of current research in this field is focused on designing more cost effective and flexible cycles for power generation. The sCO2-HeRo system however is designed to remove residual heat of nuclear fuel in the case of a station blackout with loss of the external power supply and the heat sink. The application requires that the used unrecuperated Brayton cycle is self-launching, self-propelling and self-sustaining. Furthermore, it should be possible to retrofit it to existing NPPs (Benra et al. [1]). The concept of the system is tested in the newly built sCO2 cycle at the PWR glass model at the Gesellschaft für Simulatorschulung (GfS) in Essen, Germany. The sCO2 HeRo cycle is connected to PWR glass model, which allows to demonstrate the function of the system for different emergency cases in NPPs. However, the heating power available for the demonstration cycle is only 200 kW. Compared to around 60 MW, which need to be removed in a NPP, this is rather small. It leads to a very small mass flow and consequently a very small turbomachine. As addressed by Sienicki et al. [9] all the different components of the turbomachine must be examined, when scaling turbomachines over a wide range of power output. Both the efficiency and applicability of technologies such as impellers, bearings, seals, motors, etc. must be investigated. In this paper the scaling procedure of the very small sCO2-HeRo turbomachine to the full-scale sCO2-NPP turbomachine is explained. For this purpose, both the sCO2-HeRo turbomachine and the requirements for the sCO2-NPP turbomachine are presented. The scaling procedure is described in detail with special attention to the requirements as a safety cooling system.

DESCRIPTION OF TURBOMACHINE-SET FOR THE GLASS MODEL

The turbomachine (TAC), which is implemented in the glass model, has an integrated design and consists of the three major components turbine, alternator and compressor. Figure 1 presents the cross section of the TAC with the flow directions of sCO2 and pictures of the impellers. The compressor is on the left and the turbine on the right, while the alternator is in the middle. The bearings are realized by angular hybrid ball bearings in between the impellers and the generator respectively. The thrust bearing is on the side of the compressor. Both compressor and turbine consist of one stage and have shrouded impellers with 2D-radial blading. This allows to apply labyrinth seals to reduce leakage losses. These losses have a significant influence on the components efficiency due to the small cycle mass flow. Table 1 contains the cycle mass flow and further thermodynamic conditions. The mass flow is limited by the heating power of the glass model test cycle. The maximum temperature at the turbine inlet refers to the operating conditions of the cycle in a NPP for

DOI: 10.17185/duepublico/46089

emergency cooling. The compressor inlet lies close to the critical point to reduce the compression work. For further information on the test cycle and cycle parameters please refer to Benra et al. [1]. Because of the given thermodynamic parameters and mass flow the type and dimension of the compressor and turbine (shown in Figure 1) are chosen. The nominal rotational speed of the shaft is 50,000 rpm with an electrical power of the generator of 7 kW. The cooling of the generator is realized by the compressor leakage. For more information on the TAC design and the design procedure please refer to Hacks et al.[4].

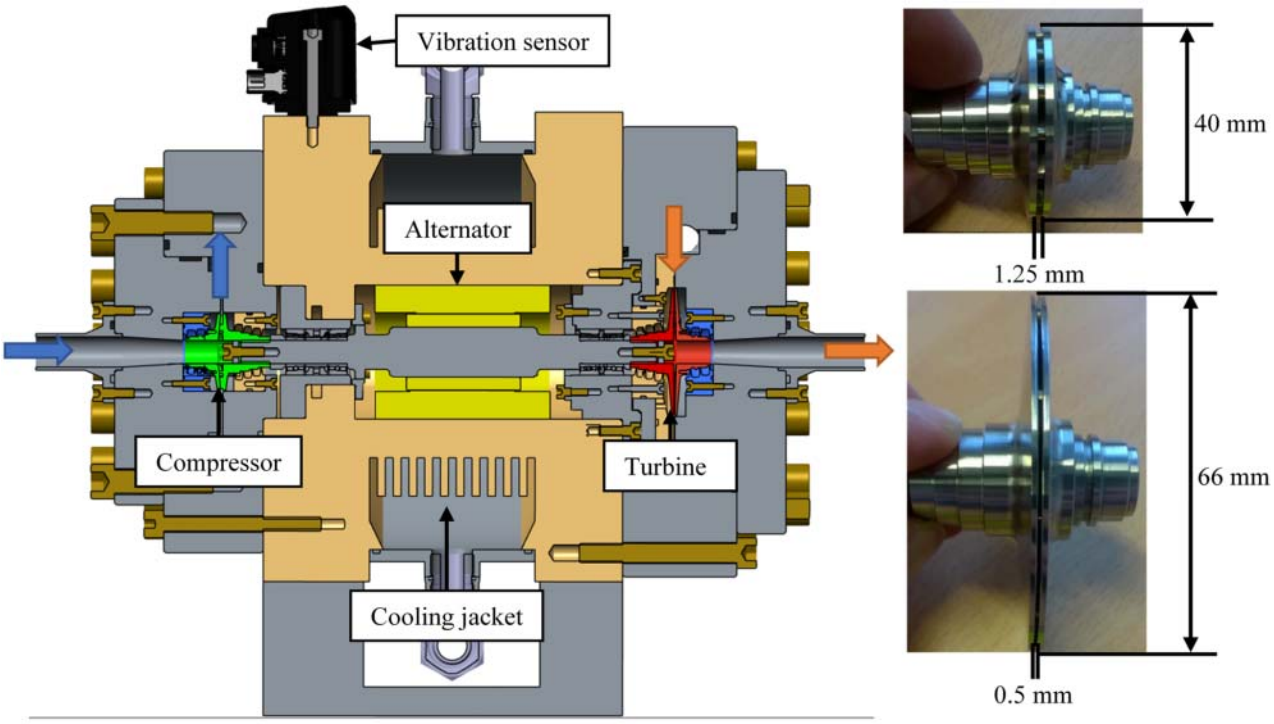

Figure 1: Cross section and impellers of the TAC with flow directions and dimensions

Table 1: Nominal conditions in the glass model

Component	Parameter	Value
Cycle	Mass flow	0.65 kg/s
Compressor inlet	Pressure*	78.3 bar
	Temperature*	33 °C
Compressor outlet	Pressure*	117.5 bar
Turbine inlet	Pressure*	117.5 bar
	Temperature*	200 °C
Turbine outlet	Pressure*	78.3 bar
Leakage	Pressure*	65 bar

*static

REQUIREMENTS TO THE TURBOMACHINE IN A NPP

The turbine inlet temperature of the sCO2-HeRo cycle is set by evaluating different options for the heat removal in an emergency case in in a NPP. Different concepts on how to remove the heat from the nuclear core were analysed resulting in different temperatures at the turbine inlet of up to 280 °C (Venker [10]). For simplification the different options of heat removal and corresponding turbine inlet temperatures are not considered, as it does not influence the general scaling procedure. It shall be assumed that the pressure and temperature of the sCO2-NPP cycle at the compressor and turbine inlet are the same as for sCO2-HeRo cycle. The amount of heat, which needs to be removed strongly depends on the size of the power plant, the time that passes after a station blackout before the sCO2-HeRo system takes over and other measures taken during that period. Venker [10] shows that the residual heat, which needs to be removed directly after the station black out, is around 60 MW_{th} for a power plant with a nominal power of around 4 GW_{th}. However, after one hour the heat drops to around 30 MW_{th} and after around 8 hours to 20 MW_{th}. The decay heat drives the sCO2-NPP cycle. The strong drop in heating power, especially in the first hours, thus request a suitable control strategy for the cycle. It is decided to divide the sCO2-NPP system in several units. Single units are then switched off step by step with decreasing decay heat. Each unit consist of one complete sCO2 cycle. The thermal energy of one sCO2-NPP unit is set to 5 MW_{th}. As the pressures and temperatures are assumed to be constant the increase in thermal power corresponds to an equivalent increase in cycle mass flow (see Figure 2). Assuming a constant pressure ratio and increased mass flow, the resulting generator power in the NPP is around 180 kW.

DOI: 10.17185/duepublico/46089

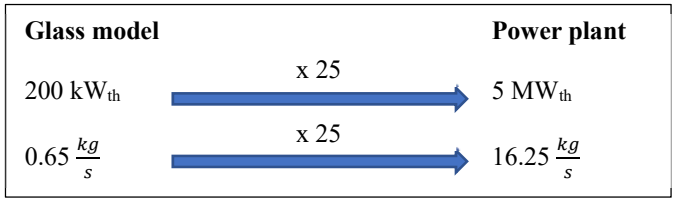

Figure 2: Mass flow – From sCO2-HeRo to sCO2-NPP size

TURBOMACHINE LAYOUT

The first thing to decide in the scaling process is whether the overall layout of the TAC is suitable for the new operation conditions. The system needs to have a simple design with a small turbomachine to retrofit existing power plants with it. The integrated design of compressor and turbine together in one casing represents the most compact machine and theoretically allows a machine without any external leakage. It is therefore desirable to keep the overall design of the sCO2-HeRo TAC as presented in Figure 1. Sienicki et al. [9] give an overview on suitable technologies for sCO2 turbomachinery in terms of size given in electrical power output. The electrical output of the sCO2-NPP turbomachine is below 1 MW$_e$, even if the thermal power per unit is raised to 10 MW$_{th}$ or 20 MW$_{th}$. According to Figure 3 the technologies applied in the sCO2-HeRo TAC, such as one stage compressor and turbine, labyrinth seals and a high-speed generator are also applicable for the sCO2-NPP machine. Thus, the integrated TAC design is considered to be suitable.

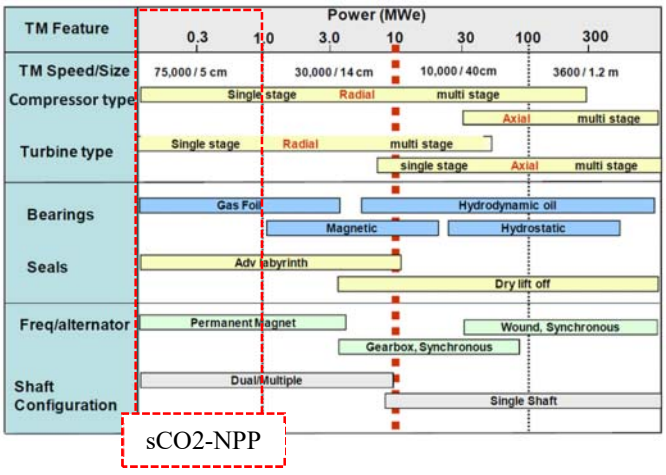

Figure 3: Technologies for sCO2 turbomachinery according to Sienicki et al. (Figure 1, [9])

AERODYNAMIC SCALING

Due to the higher mass flow the size of the TAC needs to increase. The following explanations focus on the compressor but are valid for the compressor and the turbine. A basic approach on designing a new compressor uses the Cordier diagram as presented in Figure 4. It shows the type of the impeller, and the expected efficiency of the compressor over the specific speed and specific diameter. The red dot in Figure 4 indicates the position of the sCO2-HeRo compressor. As discussed by Hacks et al. [4] the rotational speed of the compressor must be well above 150,000 rpm for the compressor to lie within a region of good efficiency because of the low mass flow. As this is not a feasible option because of excessive windage losses, the rotational speed is reduced leading to a low specific speed and large specific diameter. This causes a low flow coefficient and low efficiency according to Figure 4. A usual procedure to design a machine based on an existing design is to scale the machine according to the affinity laws. This means the machines are similar in geometry, velocities and dynamic forces (see Bohl and Elmendorf [3]). During this procedure the dimensionless parameters such as specific speed and diameter, flow and head coefficient stay constant. The scaled compressor is thus at the same position in Figure 4. As the expected efficiency is low for the sCO2-HeRo compressor (red dot), it seems not reasonable to apply scaling according to the affinity laws, but rather to shift the compressor in Figure 4 further towards higher efficiencies. To stick to the TAC design of the sCO2-HeRo with shrouded impellers and labyrinth seals, only the indicated region of radial impellers is considered (see red dotted line). To decide for the final position in Figure 4 the following influences must be considered.

1. Efficiency of the compressor and turbine
2. Windage losses
3. Leakage flow for generator cooling

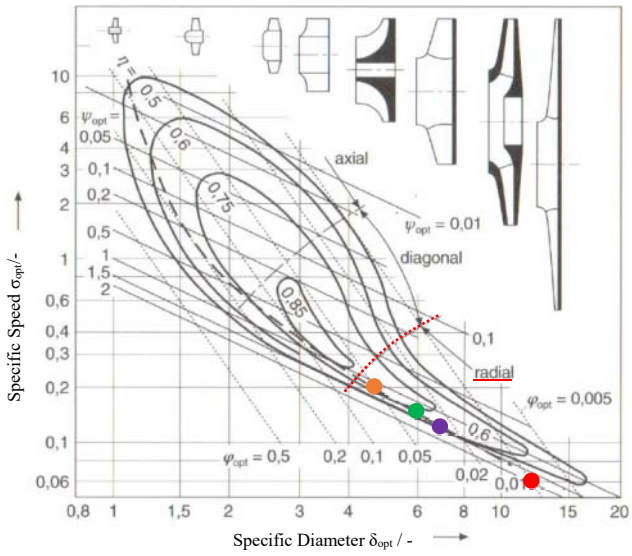

Figure 4: Cordier diagram for turbo-compressors [3][1]

[1] Labels of axes translated from German into English, Data according to Balje O. E., Turbomachines: A Guide to Design, Selection and Theory, John Wiley & Sons Inc., 1981 edited by Bohl and Elmendorf. Please note that the definition of head coefficient, specific speed and specific diameter vary from the definition of Balje by a constant factor of 2, 0.34 and 1.05 respectively.

DOI: 10.17185/duepublico/46089

The following explanations are based on the compressors and turbines given in Annex A and the motors in Annex B. Further, presented power differences are related to the power of the machine scaled by affinity laws (red dot). Because of the affinity laws, the efficiency is assumed to be the same as in the sCO2-HeRo machine and compressibility effects are neglected. All diagrams show power over rotational speed. The speed refers to a certain compressor, turbine and motor design in the tables in Annex A and Annex B. The dots that mark special operation points are presented in the following diagrams and Figure 4.

Compressor and Turbine Efficiency

As already mentioned the efficiency of compressor and turbine are expected to increase when moving the operating point along the Cordier line from the red dot towards the orange dot in Figure 4. The increase of compressor efficiency of more than 25 % from the red to the orange dot according to Figure 4 however, seems to be too large. Design CFD calculations for the sCO2-HeRo showed isentropic efficiencies of the compressor and turbine of around 66 % and 75 % already. More information on the calculations is given by Hacks et al. [4] and Schuster et al. [8]. The increase in power in Figure 4 is thus estimated by assuming a linear increase of efficiency of 5 % from the red dot towards the orange dot. This is of course a rough assumption but is deemed sufficient to present the scaling concept. Figure 5 shows that the improved efficiency causes an increase of the net-power by about 30 kW. This is caused by lower power consumption of the compressor of about 10 kW and increased turbine power of about 20 kW.

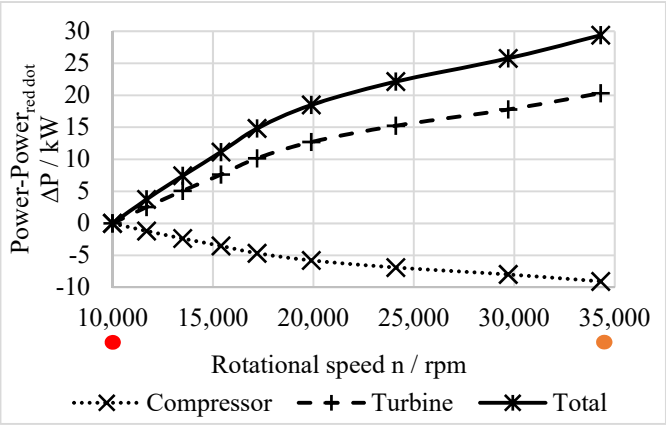

Figure 5: Power difference depended on efficiency

Windage losses

Hacks et al. [4] and others explain the high influence of windage losses on the overall efficiency of sCO2 turbomachinery. Therefore, the increased net-power must be compared to the development of the windage losses. The windage losses are determined applying the windage models of von Kármán [7] and Bilgen and Boulos [2] for the impellers and the generator respectively. The losses at the shaft seals and bearings are neglected, because they strongly depend on the chosen bearing type and shaft geometry. As direct leakage feedback without additional pump is desired and the windage losses are smaller for lower pressure, the pressure in the central housing is set to the compressor inlet pressure. The dimensions of the compressor and turbine impellers are determined using the Cordier diagram and summarized in Annex A. The motor dimensions are summarized in Annex B and retrieved using the motor type sheets of the company e+a Elektromaschinen und Antriebe AG, which supplied the motor for the sCO2-HeRo TAC. Appling equation (1) and (2) for the impeller discs indicates, that the windage losses of the impellers decrease towards higher specific speed along the Cordier line in Figure 4 (red dot towards orange dot). For the motor however, this is different. Even though the motor size decreases with increasing speed, the windage losses according to equation (3) and (4) increase. Figure 6 presents that there exists a speed, at which the windage losses reach a minimum. This speed is the optimal speed regarding windage losses, which is indicated by the purple dot in Figure 4. The losses at higher speed and smaller dimensions (orange dot) are even bigger as for the larger machine at lower speed.

Impellers:

$$c_m = \frac{0.07288}{Re^{0.2}} \tag{1}$$

$$P_{fG} = 0.5 * \pi * c_m * \rho * \omega^3 * \left(\frac{D}{2}\right)^5 \tag{2}$$

Generator:[2]

$$c_m = \frac{0.065 * \left(\frac{b}{\frac{D}{2}}\right)^{0.1}}{Re^{0.2}} \tag{3}$$

$$P_{fG} = 0.5 * c_m * \rho * \omega^3 * \left(\frac{D}{2}\right)^4 * L \tag{4}$$

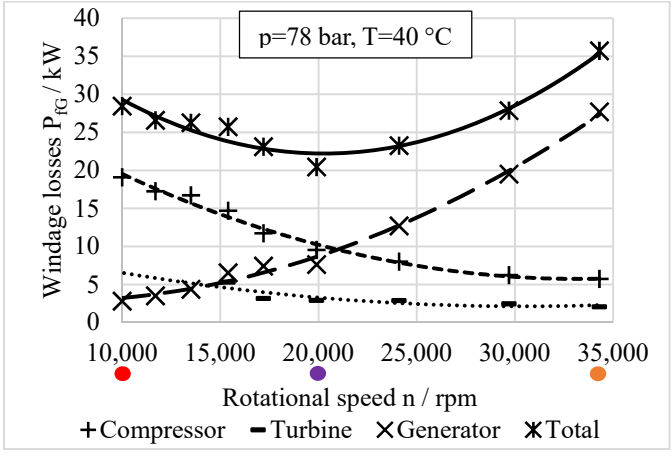

Figure 6: Windage losses at the motors and impellers

[2] Bilgen and Boulos [2] define $Re = \frac{\rho * \omega * \frac{D}{2} * b}{\mu}$. The formula for c_m is changed to fit the given definition of the Reynolds number.

DOI: 10.17185/duepublico/46089

Cooling requirements

The cooling of the generator is realized by leading the leakage of the compressor through the generator cavity and having additional cooling fins in the casing. Design calculations (see Hacks et al. [4]) and first tests showed that the concept is sufficient for generator cooling of the sCO2-HeRo TAC. Therefore, no additional cooling system is required, but a minimum leakage flow must be provided, which has influence on the compressor performance. The larger TAC has a larger generator, which produces higher power losses. The total losses of the generator consist of the previously described windage losses and the electrical losses. To approximate the required leakage flow, the necessary cooling power is calculated by equation (5). As a conservative approach the effect of the cooling fins is neglected.

$$P_{Cooling} = P_{fG} + P_{eG} \quad (5)$$

The electrical losses of the generator are approximated by the required efficiency of class IE4 of DIN EN 60034-30-1, which is 97 %. For the expected 180 kW_e of the generator this means approximately 5,4 kW of electrical losses. This represent the maximum losses, which are, for simplicity, used for all speeds. Together with the windage losses the leakage flow must remove about 3 kW to 28 kW of heat from the generator. Other windage losses along the flow path of the leakage such as the bearings and seals are neglected. To avoid large temperature gradients across the motor the maximum temperature increase of the leakage flow is set to 15 °C, which is comparable to the temperature increase in the sCO2-HeRo TAC. The inlet temperature into the cavity is 35 °C. Thus, the minimum mass flow of sCO2 to remove the heat can be approximated. It is maximally 0.5 kg/s or 3 % of the design mass flow. Hence, the influence on the overall efficiency is expected to be relatively small and generator cooling can be realized by the leakage flow. The influence on choosing the operational speed is deemed neglectable.

Scaling summary

Shifting the compressor point in Figure 4 to better efficiency causes higher rotational speed and a decreasing diameter of the impellers. Analysis of the windage losses shows, that those at the impellers decrease, while the windage losses at the generator increase. Thus, an operational speed with minimal windage losses exists. The increase in turbine and compressor efficiency causes higher shaft power. The optimal operating point is, where the power of the generator reaches its maximum. Further, the generator is cooled by the leakage flow of the compressor. Increasing windage losses require more cooling and thus a larger leakage flow from the compressor, which decreases its efficiency. It is shown that a reasonable fraction of the compressor flow is sufficient for generator cooling. Therefore, the leakage mass flow is not considered for determining the operating point. Figure 7 shows the development of the power output for different operating points. The power difference is calculated with respect to the machine, which is scaled by affinity laws having the same dimensionless parameters as the sCO2-HeRo TAC. The combination of both the development of windage losses and the power increase due to the higher compressor and turbine efficiency clearly shows an optimum operating point (green dot in Figure 7). The so found operating point is then used for detailed mechanical design of the TAC including the bearings and rotordynamics as well as blading design. As the dimensionless parameters change, it can be expected, that the sCO2-HeRo blades must be modified. Applying a 1D program considering leakage flows is required to reliably predict the compressor and turbine efficiency and power.

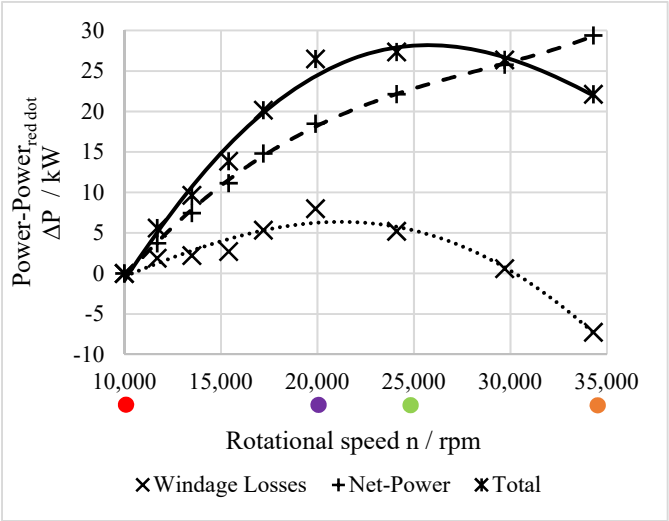

Figure 7: Development of power for different operation points

BEARINGS

The sCO2-HeRo TAC uses grease lubricated ball bearings due to size constraints and rotordynamic (see Hacks et al.[4]). First tests show that grease lubricated bearings cannot be used in sCO2 environment. Thus, a pump for pressure reduction in the central housing is required. As for a safety system in a NPP it is desirable to reduce the amount of auxiliary systems, the bearing concept needs to be changed to bearings that can operate in sCO2 environment. The characteristics of three bearing types with respect to the sCO2-NPP TAC are summarized in Table 2. As the sCO2-NPP system consist of several units, it is possible to use different strategies in the separate units. For example, very robust bearings can be used to initialise the whole system. Such bearing can be sCO2-lubricated ball bearings, which do not need to be controlled during start-up and do not have minimum speed. Therefore, they have no acceleration requirements. Initialisation means that a TAC with these bearings is used to produce little amount of electricity. The electricity then serves to start up a control system for magnetic bearings or to provide auxiliary power for rapid acceleration of the shaft using the motor for the application of gas foil bearings. As the units are switched off one after another, a machine, which employs roller bearings and thus has a low service life, is still a feasible option.

DOI: 10.17185/duepublico/46089

Table 2: Comparison of bearing concepts

	Roller bearings	Gas foil bearings	Magnetic bearings
Operating speed restrictions	Restriction of maximum speed	Need minimum speed	
Service life	Limited	Unlimited	Unlimited
Auxiliary Units	Leakage pump	Non	Control system for active control of the bearings
Design	Standard	High dependency of load capacity on fluid properties and speed	Active control of the shaft position is required
Robustness	Grease and Oil are dissolved by sCO2	Strong dependency of load capacity on fluid conditions and rotational speed	Electricity shortage means that bearings do not work (active component)
Start-Up	Allows rotation also at low speeds	Rapid start-up until minimum speed	Critical speeds can be avoided with suitable control

Roller bearings

These bearings are probably the most robust bearings as the do neither need lift-off speeds or active control. When grease or oil lubricated bearings are employed, a leakage pump is required. Initial tests of the sCO2-HeRo TAC show that, even if the grease inside the bearings is removed by sCO2, the bearings can still operate for a certain time. As the lubrication effect of the sCO2 is limited the time is short. However, the required service life for the application is maximally a few days. Thus, it seems reasonable to believe that sCO2-lubricated roller bearings can be employed if the maximum speed of the TAC and the bearing load is appropriate.

Gas foil bearings

This is the type of bearing proposed by Sienicki et al. [9] for the size range of the sCO2-NPP TAC. These bearings require a minimum lift-off speed to operate, which requires fast start-up and rapid acceleration of the shaft. Ongoing tests of the sCO2-HeRo address the start-up of the system to determine the required time and procedure. The load capacity of the bearings is strongly dependent on the rotational speed and very limited at low speed. The bearings therefore need to be carefully designed and the operation range must be set leaving sufficient margin towards higher loads and low speeds to allow save operation. Additionally, the gap between the stator and rotor parts is very narrow causing high losses when operated in sCO2. The key advantage for the safety system is, that gas foil bearings can operate without additional auxiliary units and without wearing off.

Magnetic bearings

These bearings need to be controlled when in operation and thus need a fully operational control system during start-up of the safety system. They need to be as carefully designed as foil bearings but allow a wider operation range regarding rotational speed. This means, that they do not need a minimum speed to operate and are additionally able to actively avoid critical speeds by altering their stiffness and damping behaviour. Further the gap between rotor and stator is larger as for gas foil bearings causing lower losses. The service life is basically unlimited. As a loss of the control system makes the bearings stop working, additional catcher bearings such as non-lubricated ball bearings must be employed to safe the shaft from falling into the stator.

ROTORDYNAMICS

Finally, also rotordynamics need to be considered. The increasing speed means that during start-up critical speeds need to be considered. For the application as safety system generally a wide range of operational speed with low influence of critical speeds is desired. The generated electrical power is not the key requirement of the cycle. Therefore, it might be better to stick to low rotational speeds, even if the efficiency is lower. If the bearing system is known rotordynamic considerations such as avoiding critical speeds can directly be included in the process of choosing an operational speed. As this is not yet the case for the sCO2-NPP system it is not considered in this paper.

CONCLUSION

It is presented, that for the scaled sCO2-NPP TAC the same design approach can be used as for the sCO2-HeRo TAC. Scaling following the affinity laws means that the efficiency of the sCO2-NPP TAC is low. To increase efficiency the operating point can be shifted in the Cordier diagram. The operating point is found by iterative calculation and comparison of the compressor and turbine efficiency and the windage losses. The cooling requirement is manly dependent on the windage losses. The required leakage flow for generator cooling is small compared to the main flow in the cycle. Therefore, it is not necessary to consider it for choosing the operation point. More detailed calculations such as rotordynamics, which consider the operational restrictions such as critical speeds can be included, too. For this it is necessary to define the appropriate bearing type. The sCO2-NPP TAC shall operate with sCO2 in the central housing. Different bearing types are compared with considering the requirements of the safety system. The most appropriate bearing type is dependent on the machine behaviour and control strategy especially during start-up. This is subject to the ongoing tests of the sCO2-HeRo TAC and no decision can be made yet.

DOI: 10.17185/duepublico/46089

NOMENCLATURE

Symbol	Unit	Description
b	m	Cavity height
c_m	-	Moment coefficient
D	m	Diameter
L	m	Length
$\dot{m}$	kg/s	Mass flow
n	1/s	Rotational speed
P	kW	Power
Q	m³/s	Volume flow
$Re = \frac{\rho * \omega * \left(\frac{D}{2}\right)^2}{\mu}$		
u	m/s	Circumferential speed
y	J/kg	Specific flow work
$\delta_{opt} = \frac{\psi_{opt}^{\frac{1}{4}}}{\sqrt{\varphi_{opt}}} = D * \sqrt[4]{\frac{2*y}{Q^2}} * \frac{\sqrt{\pi}}{2}$	-	Specific diameter
η	%	Isentropic Efficiency
μ	Pa*s	Dynamic viscosity
ρ	kg/m³	Density
$\sigma_{opt} = \frac{\sqrt{\varphi_{opt}}}{\psi_{opt}^{\frac{3}{4}}} = n * \frac{2*\sqrt{\pi}*\sqrt{Q}}{(2*y)^{\frac{3}{4}}}$	-	Specific speed
$\varphi_{opt} = \frac{c_m}{u} = \frac{4*Q}{\pi^2*D^3*n}$	-	Flow coefficient
$\psi_{opt} = \frac{2*y}{u^2} = \frac{2*y}{\pi^2*D^2*n^2}$	-	Head coefficient
ω	Rad/s	Angular speed

Abbreviation	Description
BWR	Boiling water reactor
GfS	Gesellschaft für Simulatorschulung mbH
NPP	Nuclear power plant
PWR	Pressurized water reactor
sCO2	Supercritical CO_2
sCO2-HeRo	The supercritical CO_2 heat removal system for the glass model
sCO2-NPP	The supercritical CO_2 heat removal system for a nuclear power plant
TAC	Turbine, alternator, compressor system

Subscript	Description
e	Electrical
f	Friction
G	Generator
th	Thermal

ACKNOWLEDGEMENTS

This project has received funding from the European research and training programme 2014 – 2018 under grant agreement No 662116.

REFERENCES

[1] Benra, F.-K., Brillert, D., Frybort, O., Hajek, P., Rohde, M., Schuster, S., Seewald, M. & Starflinger, J. (2016). A supercritical CO2 low temperature Brayton-cycle for residual heat removal. *The 5th International Symposium - Supercritical CO2 Power Cycles*, San Antonio, Texas, USA

[2] Bilgen, E. & Boulos, R. (1973). Functional Dependence of Torque Coefficient of Coaxial Cylinders on Gap Width and Reynolds-Numbers. *Journal of Fluids Engineering*, 95(1), 122-126

[3] Bohl, W. & Elmendorf, W. (2013). *Strömungsmaschinen 1. Aufbau und Wirkungsweise* (Vol. 11), Würzburg: Vogel

[4] Hacks, A. J., Schuster, S., Dohmen H. J., Benra F.-K. & Brillert D. (2018). Turbomachine Design for Supercritical Carbon Dioxide within the sCO2-HeRo.eu Project. *ASME Turbo Expo*, Oslo, Norway

[5] e+a Elektromaschinen und Antriebe AG (2017). Asynchron-Elan types – 4-pole – 08/2017

[6] e+a Elektromaschinen und Antriebe AG (2017). Asynchron-Standard types – 4 pole – 06/2017

[7] Kármán, Th v. (1921) Über laminare und turbulente Reibung. *ZAMM-Journal of Applied Mathematics and Mechanics/Zeitschrift für Angewandte Mathematik und Mechanik*, 1(4), 233-252.

[8] Schuster S., Benra F.-K., Brillert D. (2016) Small scale sCO2 compressor impeller design considering real fluid conditions. *The 5th International Symposium - Supercritical CO2 Power Cycles*, San Antonio, Texas, USA

[9] Sienicki, J. J., Moisseytsev, A., Fuller, R. L. Wright, S. A. & Pickard, P. S. (2011). Scale Dependencies of Supercritical Carbon Dioxide Brayton Cycle Technologies and the Optimal Size for a Next-Step Supercritical CO2 Cycle Demonstration. *SCO2 Power Cycle Symposium*, Boulder, Colorado, USA

[10] Venker, J. (2015). Development and validation of models for simulation of supercritical carbon dioxide Brayton cycles and application to self-propelling heat removal systems in boiling water reactors. *IKE (Institut für Kernenergetik und Energiesysteme), Universität Stuttgart*, Stuttgart, Germany

DOI: 10.17185/duepublico/46089

ANNEX A

COMPRESSOR AND TURBINE PARAMETERS

The compressor and turbine parameters are determined with help of the Cordier diagram. First the dimensionless parameters of the compressor are read out of the Cordier diagram along the Cordier line from the red to the orange dot in Figure 4. Then diameter and speed are calculated by the given formulas. Secondly the dimensionless turbine parameters are determined for rotational speeds calculated before. The Cordier line for turbines on page 79 in the book of Bohl and Elmendorf [3] is used. The pressure ratio and inlet conditions are assumed to be constant. The highlighted points in the Figure 4 to Figure 7 are marked. Additionally, the tables contain the compressor and turbine data for all other points shown in the diagrams Figure 5 to Figure 7 marked as support points.

Table 3: Comparison of the basic parameters of the compressor

Position in Figure 4	**Rotational speed n (rpm)**	**Impeller Diameter D (mm)**	**Mass Flow ṁ (kg/s)**	**Isentropic Efficiency η (%)**	**Specific diameter δ_{opt} (-)**	**Specific speed σ_{opt} (-)**	**Flow coefficient φ_{opt} (-)**	**Head coefficient ψ_{opt} (-)**
sCO2-HeRo	50,000	40	0.65	66.3	12.4	0.06	0.009	1.8
Red dot (scaled by affinity laws)	10,000	200	16.25	66.3	12.4	0.06	0.009	1.8
Support point	11,600	178	16.25	66.8	11	0.07	0.011	1.7
Support point	13,400	162	16.25	67.3	10	0.08	0.012	1.5
Support point	15,100	146	16.25	67.8	9	0.09	0.015	1.4
Support point	16,800	130	16.25	68.3	8	0.10	0.019	1.4
Purple dot	19,400	114	16.25	68.8	7	0.12	0.024	1.4
Green dot	23,300	98	16.25	69.3	6	0.15	0.032	1.3
Support point	28,600	82	16.25	69.8	5	0.18	0.045	1.2
Orange dot	32,800	74	16.25	70.3	4.5	0.21	0.053	1.1

Table 4: Comparison of the basic parameters of the turbine

Position in Figure 4	**Rotational speed n (rpm)**	**Impeller Diameter D (mm)**	**Mass Flow ṁ (kg/s)**	**Isentropic Efficiency η (%)**	**Specific diameter δ_{opt} (-)**	**Specific speed σ_{opt} (-)**	**Flow coefficient φ_{opt} (-)**	**Head coefficient ψ_{opt} (-)**
sCO2-HeRo	50,000	66	0.65	74.8	10.9	0.07	0.011	1.6
Red dot (scaled by affinity laws)	10,000	330	16.25	74.8	10.9	0.07	0.011	1.6
Support point*	11,600	282	16.25	75.3	9.3	0.09	0.015	1.6
Support point*	13,400	231	16.25	75.8	7.6	0.10	0.023	1.8
Support point*	15,100	181	16.25	76.3	6	0.11	0.042	2.3
Support point	16,800	151	16.25	76.8	5	0.12	0.066	2.7
Purple dot	19,400	135	16.25	77.3	4.5	0.14	0.079	2.6
Green dot	23,300	120	16.25	77.8	4	0.17	0.094	2.3
Support point	28,600	102	16.25	78.3	3.4	0.20	0.125	2.1
Orange dot	32,800	90	16.25	78.8	3	0.23	0.160	2.1

*Extrapolated from Cordier diagram

DOI: 10.17185/duepublico/46089

ANNEX B

MOTOR SIZES

Table 5 contains the rotor diameter and length including the end rings for different rotational speeds. The motor parameters were extracted from the type overview of 4 pole asynchronous motors (see [5] and [6]) and the "Motor Scout" offered by e+a Elektromaschinen und Antriebe AG for an approximated power of 180 kW. The outer rotor diameter is approximated by the inner stator diameter. The rotor length is calculated from the stator stack length, determined using the "Motor Scout" of e+a Elektromaschinen und Antriebe AG according to the names in Table 5, and the rotor ring length in the type overview.

Table 5: Motor Sizes for the determination of windage losses in Figure 6

Speed (rpm)	Name	Outer Rotor Diameter (mm)	Total Rotor Length (mm)
10,000	mW 20/36-4-s2r5	130	396
11,600	mW 20/26-4-s3r3	130	296
13,400	mW 20/26-4-s3r3	130	296
15,100	mW 20/26-4-s3r3	130	296
16,800	mW 17/40-4-s2r5	110	432
19,400	mW 17/25-4-s2r5	110	282
23,300	mW 17/25-4-s2r5	110	282
28,600	mW 17/20-4-s2r5*	110	232
32,800	mW 17/20-4-s2r5*	110	232

* Maximum speed of the motor is 29,000 rpm. No motors are available in the type overview for speeds above 29,000 rpm.

DOI: 10.17185/duepublico/46089